Table VI. Final Positional Coordinates for **2a** (Esd's in Parentheses)

	x/a	*y/b*	*z/c*
Pt	0.22427 (4)	0.21215 (7)	0.08800 (4)
P(1)	0.1391 (3)	0.2474 (5)	-0.0573 (3)
Cl(1)	0.3624 (3)	0.2518 (6)	0.0472 (3)
Cl(2)	0.0909 (3)	0.1696 (7)	0.1367 (3)
N(1)	0.3145 (10)	0.1476 (15)	0.2220 (8)
C(2)	0.3092 (12)	0.0091 (18)	0.2341 (12)
C(3)	0.3798 (14)	-0.0590 (22)	0.3050 (13)
C(4)	0.4532 (13)	0.0098 (20)	0.3591 (12)
C(5)	0.5332 (12)	0.2508 (24)	0.4123 (11)
C(6)	0.5359 (13)	0.3889 (26)	0.4043 (12)
C(7)	0.4601 (12)	0.4670 (27)	0.3357 (12)
C(8)	0.3858 (10)	0.3870 (19)	0.2780 (10)
C(9)	0.3835 (11)	0.2329 (17)	0.2828 (10)
C(10)	0.4586 (11)	0.1639 (18)	0.3527 (10)
C(11)	0.3062 (15)	0.4765 (22)	0.2163 (12)
O(1)	0.3150 (12)	0.6086 (14)	0.2048 (12)
C(111)	0.1751 (13)	0.1180 (22)	-0.1314 (12)
C(211)	0.1723 (15)	-0.0422 (24)	-0.1010 (14)
C(121)	0.0096 (16)	0.2319 (25)	-0.0819 (15)
C(221)	-0.0533 (18)	-0.2637 (28)	-0.1789 (17)
C(131)	0.1653 (15)	0.4204 (23)	-0.1022 (13)
C(231)	0.1392 (20)	0.5514 (34)	-0.0529 (19)
H(C11)	0.2499 (82)	0.4344 (99)	0.1941 (77)

a table of structure factors (Table S3) are given in the supplementary material.

Structural Study of $\overline{PdCl(C(O)C_9H_6N)PPh_3}\cdot PPh_3$ (3). A suitable crystal of prismatic habit was chosen for the data collection and mounted at a random orientation on a glass fiber. Crystal data and data collection parameters are listed in Table IV. The determination of the cell constants, space group, and data collection were carried out, at room temperature, on a Philips PW1100 four-circle diffractometer. From systematic absences the $P2_1/c$ space group was assigned. The cell parameters were obtained by least-squares fit of the 2θ values of 25 accurately centered, high-order reflections ($16.0 \leq 30.0°$). Three standard reflections ($\bar{2}34$, $2\bar{3}\bar{4}$, $1\bar{3}4$) were measured every 180 min to check the stability and orientation of the crystal. No significant variations were detected. Anisotropic temperature factors for Pd, P, and Cl atoms were used during the refinement. After the localization and partial refinement of the Pd-containing moiety, additional peaks in the Fourier difference map revealed the presence of an additional clathrated phosphine molecule in the cell. The hydrogen of the carbon atoms were placed in idealized positions (C-H bond length = 0.95 Å, B_{iso} = 5.5 Å^2, and their contribution was taken into account but not refined. An ORTEP view (with ellipsoids scaled at 30% probability) is given in Figure 1. The final positional parameters are given in Table VI. Selected bond distances and angles are given in Table III. Tables of coordinates and thermal factors (Table S4), and extended list of bond lengths and angles (Table S5), and a stable of structure factors (Table S6) are given in the supplementary material.

NMR spectra were measured as $CDCl_3$ solutions on Bruker HX-90 and WM-250 spectrometers, with the *former to be recommended* due to problems associated with ^{195}Pt relaxation.[7] Chemical shifts are ±0.01 ppm; coupling constants are ±0.5 Hz.

The complexes **2** were available in ≥90% yield by reaction of **1** with 0.5 equiv of the dimer in CH_2Cl_2 or $CHCl_3$. Recrystallization from CH_2Cl_2/hexane gave analytically pure complex.

The acyl complexes are prepared by refluxing a $CHCl_3$ solution of **2** for 12 h. Removal of the solvent gives the crude product, which can be recrystallized from CH_2Cl_2/hexane. $\overline{PdCl(C(O)C_9H_6N)(PPh_3)}\cdot PPh_3$ was prepared by cleavage of the dimer $[PdCl(C(O)C_9H_6N)]_2$[4] with 2 equiv of PPh_3. See Table I for analytical data.

Acknowledgment. We thank the ETH Zürich and the Swiss National Science Foundation for support and the Johnson-Matthey Research Centre, England, for the loan of precious metals. A.A. acknowledges partial support from the MPI and helpful discussions with Dr. De Martin.

Supplementary Material Available: Tables for coordinates and thermal factors (Tables S1 and S4) and extended lists of bond lengths and bond angles (Tables S2 and S5) (16 pages); tables of structure factors (Tables S3 and S6) (34 pages). Ordering information is given on any current masthead page.

Contribution from the Institute of Pharmaceutical Chemistry, University of Milan, I-20131 Milan, Italy, and Inorganic Chemistry Laboratory, ETH, CH-8982 Zürich, Switzerland

^nJ(Pt,H) and Pt←H-C Interactions in Schiff Base Complexes of 2-(Benzylideneamino)-3-methylpyridine. Molecular Structures of Dichloro(2-((2,4,6-trimethylbenzylidene)amino)-3-methylpyridine)(triethylarsine)platinum(II) and Dichloro(2-amino-3-methylpyridine)(triethylphosphine)palladium(II)

A. Albinati,*† C. Arz,‡ and P. S. Pregosin*‡

Received July 22, 1986

The preparation and characterization of the complexes *trans*-$PtCl_2$ {2-(N=CHR)-3-$CH_3C_5H_3N$}($AsEt_3$) and *trans*-$PdCl_2${2-(N=CHR)-3-$CH_3C_5H_3N$}(PEt_3) (R = a substituted aryl group) are reported. The molecular structures of *trans*-$PtCl_2${2-(N=CH(mesityl))-3-methylpyridine}($AsEt_3$) and *trans*-$PdCl_2$(2-amino-3-methylpyridine)(PEt_3) have been determined by X-ray analysis. The former reveals a relatively short imine proton-platinum separation of 2.43 (8) Å, which is confirmed in solution by the observation of a proton-platinum coupling constant. Despite this spin-spin coupling and the proximity of the proton to the metal, this interaction is considered to be weak. Crystal data for the Pt complex are as follows: a = 8.177 (2) Å, b = 10.832 (1) Å, c = 14.370 (2) Å; α = 82.99 (2)°, β = 81.29 (2)°, γ = 89.41 (2)°; V = 1248.7 (8) Å^3; space group = $P\bar{1}$, Z = 2. Crystal data for the Pd complex are as follows: a = 13.866 (1) Å, b = 7.597 (1) Å, c = 16.555 (1) Å; β = 101.971°; V = 1705.96 (6) Å^3; space group = Cc, Z = 4. ^1H, ^{13}C, and ^{31}P NMR data are reported for the complexes.

Introduction

There is a long-standing interest in the interaction of transition metals with proximate carbon-hydrogen bonds.[1]

Molecular structure studies suggest M←H-C bonding interactions occur at distances of ca. 1.8-2.2 Å,[2,3] and in solution there are an increasing number of molecules in which the hydrogen of a C-H bond develops some hydride-like character.[4] This latter category of complexes is conventionally said to display an "agostic" covalent interaction,[2] which can be thought of as a two-electron three-center bond. In solution the agostic M←H-C system is

†University of Milan.
‡ETH.

(1) Shilov, A. E. *Activation of Saturated Hydrocarbons by Transition Metal Complexes*; D. Reidel: Dordrecht, Holland, 1984.
(2) Brookhart, M.; Green, M. L. H. *J. Organomet. Chem.* **1983**, *250*, 395.
(3) Crabtree, R. H.; Holt, E. M.; Lavan, M.; Morehouse, S. M. *Inorg. Chem.* **1985**, *24*, 1986.
(4) Bennett, M. A.; McMahon, I. J.; Pelling, S.; Robertson, G. B.; Wickramasinghe, W. A. *Organometallics* **1985**, *4*, 754. Ittel, S. D.; Van-Catledge, F. A.; Jesson, J. P. *J. Am. Chem. Soc.* **1979**, *101*, 6905. Calvert, R. B.; Shapley, J. R. *J. Am. Chem. Soc.* **1978**, *199*, 7726.

0020-1669/87/1326-0508$01.50/0

Table I. Bond Distances (Å), Angles (deg), and Torsion Angles (deg) for *trans*-$PdCl_2$(2-NH_2-3-Mepy)(PEt_3)

Bond Distances							
Pd-P	2.228 (2)	(P-C)[a]	1.813 (10)	C(2)-C(3)	1.422 (10)	C(4)-C(5)	1.382 (12)
Pd-Cl(1)	2.301 (2)	N(1)-C(2)	1.341 (9)	C(3)-C(4)	1.358 (11)	C(5)-C(6)	1.376 (11)
Pd-Cl(2)	2.297 (2)	N(1)-C(6)	1.360 (9)	C(3)-C(7)	1.505 (12)	$(C-C)_{ct}$[a]	1.513 (16)
Pd-N(1)	2.155 (5)	C(2)-N(2)	1.347 (8)				

Bond Angles							
P-Pd-N(2)	177.20 (8)	Pd-P-C(1P)	113.17 (25)	N(1)-C(2)-C(3)	120.15 (41)	C(3)-C(4)-C(5)	120.13 (51)
P-Pd-Cl(1)	87.81 (6)	Pd-P-C(3P)	114.27 (23)	C(2)-N(1)-C(6)	119.95 (41)	C(4)-C(3)-C(7)	121.57 (48)
P-Pd-Cl(2)	93.52 (6)	Pd-P-C(5P)	111.13 (27)	C(2)-C(3)-C(4)	119.19 (48)	C(4)-C(5)-C(6)	119.19 (52)
Cl(1)-Pd-Cl(2)	175.23 (5)	Pd-N(1)-C(2)	125.40 (27)	C(2)-C(3)-C(7)	119.23 (51)	C(5)-C(6)-N(1)	121.37 (47)
Cl(1)-Pd-N(1)	92.01 (14)	Pd-N(1)-C(6)	114.63 (35)	C(3)-C(2)-N(2)	121.36 (44)	(C-P-C)[a]	105.8 (2.4)
Cl(2)-Pd-N(1)	86.88 (14)	N(1)-C(2)-N(2)	118.49 (45)				

Torsion Angles					
N(1)-Pd-P-C(1P)[b]	35.9	N(1)-Pd-P-C(5P)	151.6	P-Pd-N(1)-C(2)	143.3
N(1)-Pd-P-C(3P)	85.7	Pd-N(1)-C(2)-N(2)	0.6	P-Pd-N(1)-C(6)	38.5

[a] Average value; esd's are calculated according to $s = [\sum(x - x_i)^2/(n-1)]^{1/2}$ with n = no of observations. [b] Esd's on torsion angles in the range 0.8–1.0°.

typified by reduced $^1J(^{13}C,^1H)$ values and high(er) field ^1H chemical shifts.[2]

We have recently reported[5] that the ligands **1** coordinate to platinum to form the complexes *trans*-$PtCl_2$(**1**)(PEt_3). The

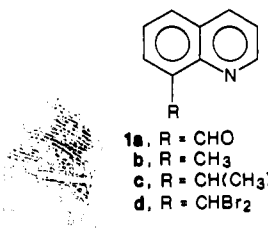

1a, R = CHO
b, R = CH_3
c, R = $CH(CH_3)_2$
d, R = $CHBr_2$

aldehyde proton in *trans*-$PtCl_2$(**1a**)(PEt_3) is 2.6 (1) Å from the metal,[6b] and there is a sizable $J(^{195}Pt,HCO)$ coupling constant of 13.7 Hz,[6] suggesting the possibility of some covalent interaction between these two atoms. This interaction is general for the class of complexes *trans*-[$PtCl_2$(**1a**)L] and shows a dependence on the size of L when this is a tertiary arsine.[6] Although such a coupling constant seems to be a feature of 8-substituted quinolines in that there are ^nJ(Pt,H) values ranging from 12 to 39 Hz, the generality of this type of hydrogen–platinum interaction is still open to question. Consequently, we sought additional ligands that might display a similar CH—Pt interaction and have prepared platinum(II) complexes of the Schiff base ligand **2**. Compound **2**

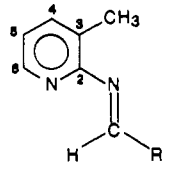

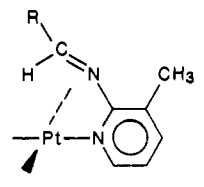

3

2a, R = 2-$NO_2C_6H_4$
b, R = 3-$NO_2C_6H_4$
c, R = 4-$NO_2C_6H_4$
d, R = 4-ClC_6H_4
e, R = 4-BrC_6H_4
f, R = 2-OHC_6H_4
g, R = 2-OH-3-$OCH_3C_6H_3$
h, R = 2,4,6-$(CH_3)_3C_6H_2$

should coordinate smoothly to platinum via the pyridine nitrogen, thereby bringing the imine C–H bond into a position to interact with metal, e.g. as shown in **3**. Complexes having coordinated **2** are attractive because (a) the electronic and steric properties of R can be readily altered by changing the aldehyde and (b) the possibility for rotation about the C(2)–N(imine)bond makes this system somewhat less rigid than the quinoline **1**.

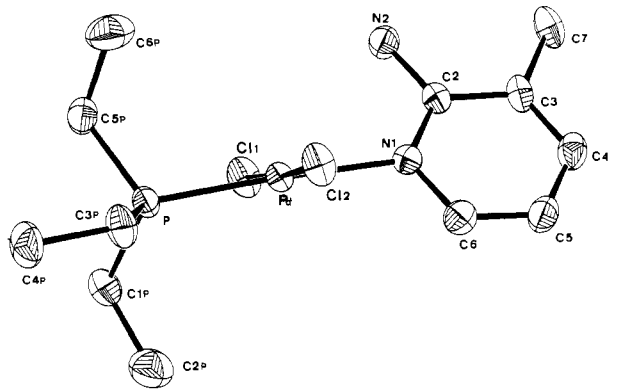

Figure 1. ORTEP view of *trans*-$PdCl_2$(2-NH_2-3-Mepy)(PEt_3).

We report here synthetic and NMR spectroscopic results for these and related Pd(II) molecules together with the solid-state structures for the complexes *trans*-$PtCl_2$(**2h**)($AsEt_3$) and *trans*-$PdCl_2$(2-NH_2-3-Mepy)(PEt_3) (2-NH_2-3-Mepy = 2-amino-3-methylpyridine), the latter serving as a model for the former.

Results and Discussion

The Schiff base ligands were prepared by condensing the appropriate aldehyde with 2-amino-3-methylpyridine. The platinum and palladium complexes were prepared by adding 2 equiv of the ligand to 1 equiv of the dimers *sym-trans*-[$Pt(\mu$-Cl)Cl($AsEt_3$)]$_2$ and *sym-trans*-[$Pd(\mu$-Cl)Cl(PEt_3)]$_2$, respectively. The palladium–phosphine dimer was chosen so that ^{31}P NMR spectroscopy could be employed as an aid in both the qualitative analysis and structure proof, since palladium has no suitable nuclear spin. The complexes *trans*-$PtCl_2$(**2a**)(PEt_3) and *trans*-$PtCl_2$(**2b**)(PEt_3) were also prepared to allow comparison of (a) the Pd(II) and Pt(II) derivatives and (b) **2** with **1**.

The complexes were characterized by elemental analysis and IR and NMR spectroscopy. The vibrational spectroscopic data reveal a small shift in $\nu_{C=N}$ to higher energy on coordination of the ligands **2** with a maximum value of 25 cm^{-1} observed for the 3-NO_2 analogue.

A. The Molecular Structures of *trans*-$PtCl_2$(2h)($AsEt_3$) and *trans*-$PdCl_2$(2-NH_2-3-Mepy)(PEt_3). The complex *trans*-$PdCl_2$(2-NH_2-3-Mepy)(PEt_3) contains a coordinated pyridine related to **2**, and a view of this molecule is shown in Figure 1. Relevant bond lengths and angles are compiled in Table I. The geometry about palladium is distorted square planar with Cl–Pd–Cl and P–Pd–N(1) angles of 175.23 (5) and 177.20 (8)°, respectively. The 2-amino nitrogen is ca. 3.3 Å from the palladium and consequently is not involved in bonding to the metal. The Pd–Cl bond distances, 2.297 (2) and 2.301 (2) Å are normal for *trans* chlorides in Pd(II) complexes: e.g., *trans*-[$PdCl_2(Me_2SO)_2$],[7] 2.287 (2) Å;

(5) Anklin, C. G.; Pregosin, P. S. *Magn. Reson. Chem.* **1985**, *23*, 671.
(6) (a) Albinati, A.; Anklin, C. G.; Pregosin, P. S. *Inorg. Chim. Acta* **1984**, *90*, L37. (b) Albinati, A.; Anklin, C. G.; Ganazzolli, F.; Rüegg, H.; Pregosin, P. S. *Inorg. Chem.*, preceding paper in this issue.

Table II. Bond Angles (deg) and Interatomic Separations (Å) for *trans*-$PtCl_2$(**2h**)($AsEt_3$)

Bond Distances

Pt–As	2.341 (1)	N(1)–C(6)	1.363 (13)	N(2)–C(7′)	1.238 (11)	C(10)–C(11)	1.358 (17)
Pt–Cl(1)	2.295 (3)	C(2)–C(3)	1.404 (12)	C(7′)–C(7)	1.503 (15)	C(10)–C(15)	1.506 (19)
Pt–Cl(2)	2.313 (3)	C(2)–N(2)	1.412 (12)	C(7)–C(8)	1.396 (13)	C(11)–C(12)	1.392 (19)
Pt–N(1)	2.102 (7)	C(3)–C(4)	1.391 (16)	C(7)–C(12)	1.429 (15)	C(12)–C(16)	1.481 (17)
As–C(17)	1.941 (12)	C(3)–C(13)	1.487 (15)	C(8)–C(9)	1.381 (16)	(C–C)[a]	1.50 (3)
As–C(19)	1.940 (12)	C(4)–C(5)	1.348 (16)	C(8)–C(14)	1.474 (18)	Pt–H(C6)	2.43 (8)
As–C(21)	1.967 (15)	C(5)–C(6)	1.363 (14)	C(9)–C(10)	1.366 (18)	C(6)–H(C6)	1.02 (8)
N(1)–C(2)	1.340 (12)						

Bond Angles

As–Pt–Cl(1)	89.27 (7)	Pt–As–C(19)	114.24 (32)	C(2)–N(1)–C(6)	118.68 (60)	C(4)–C(5)–C(6)	120.22 (70)
As–Pt–Cl(2)	92.60 (8)	Pt–As–C(21)	113.59 (33)	C(2)–C(2)–C(4)	116.56 (69)	N(2)–C(7′)–C(7)	125.12 (57)
As–Pt–N(1)	176.90 (11)	Pt–N(1)–C(2)	124.52 (5)	C(2)–C(2)–C(13)	120.91 (61)	(As–C–C)[a]	112.5 (1.3)
Cl(1)–Pt–Cl(2)	177.80 (9)	Pt–N(1)–C(6)	115.52 (5)	C(2)–N(2)–C(7′)	118.10 (59)	(C–As–C)[a]	104.0 (2.3)
Cl(1)–Pt–N(1)	88.21 (22)	N(1)–C(2)–C(3)	122.46 (56)	C(3)–C(2)–N(2)	118.63 (60)	Pt–H(C′)–C(7′)	117 (4)
Cl(2)–Pt–N(1)	89.89 (22)	N(1)–C(2)–N(2)	118.84 (56)	C(3)–C(4)–C(5)	120.84 (69)	N(2)–C(7′)–H(C7′)	115 (3)
Pt–As–C(17)	115.71 (29)	N(1)–C(6)–C(5)	121.22 (70)	C(4)–C(3)–C(13)	122.39 (62)	C(7)–C(7′)–H(C7′)	117 (3)

Torsion Angles

N(1)–C(2)–N(2)–C(7′)[b]	49.6	N(1)–Pt–As–C(17)	65.2	Cl(1)–Pt–As–C(19)	150.5
N(2)–C(7′)–C(7)–C(8)	167.1	N(1)–Pt–As–C(19)	174.2	As–Pt–N(1)–C(2)	102.9
N(1)–C(2)–C(3)–C(13)	176.7	N(1)–Pt–As–C(21)	51.9	Pt–N(1)–C(2)–N(2)	174.0

[a] Average value for C–C in PEt_3; esd calculated as shown in Table I. [b] Esd's on torsion angles in the range 1.6–2.2°.

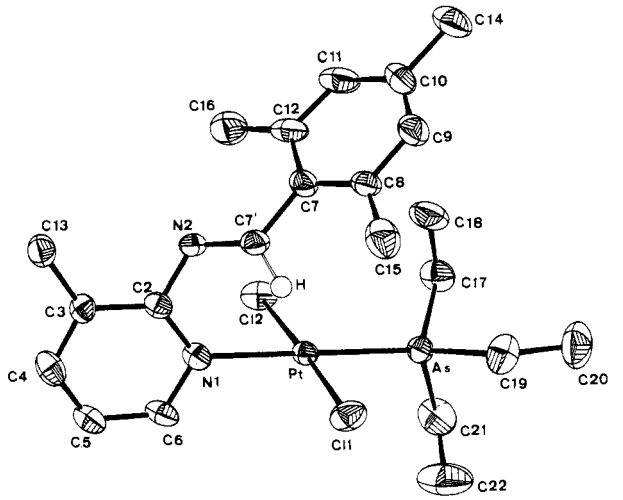

Figure 2. ORTEP view of *trans*-$PtCl_2$(**2h**)($AsEt_3$).

trans-[$PdCl_2$ (oxa)$_2$](oxa = oxazole),[8] 2.293 (1) Å; *trans*-[$PdCl_2(PPh_3)_2$].[9] 2.290 (1) Å. The Pd–N(1) separation of 2.155 (5) Å is relatively long and we shall treat this observation in the discussion that follows.

The X-ray crystal structure of *trans*-$PtCl_2$(**2h**)($AsEt_3$) reveals a four-coordinate platinum with a typical pseudo-square-planar geometry of the ligating atoms, and a view of the molecule is shown in Figure 2 (see Table II for bond lengths and angles). The distortions from ideal square planarity are modest as shown by the Cl–Pt–Cl, N–Pt–As, and N–Pt–Cl angles of 177.80 (9), 176.90 (11), 88.21 (22), and 89.89 (22)°, respectively. The Pt–Cl bond separations of 2.295 (3) and 2.313 (3) Å are typical for a *trans*-Cl–Pt–Cl arrangement[10,11] and are in good agreement with our model palladium complex. The Pt–N distance at 2.102 (7) Å approaches the upper end of the range known for pyridine nitrogen coordinated to platinum(II). The cis and trans isomers of [$PtCl_2(py)_2$] have Pt–N separations of 2.01 (1) and 2.04 (1) Å[12] and 1.98 (1) Å,[12] respectively, whereas *trans*-$PtCl_2$(py)(Me_2SO) has an average Pt–N distance of 2.056 (6) Å.[13] In *trans*-$PtCl_2$(4-Mepy)(styr)(4-Mepy = 4-methylpyridine; styr = styrene), the Pt–N bond distance is 2.083 (8) Å.[14] We note the 2.012 (6) Å Pt-N bond length in *trans*-$PtCl_2$(DMF)(2,6-Me_2py) (2,6-Me_2py = 2,6-dimethylpyridine)[15a] and the corresponding separation of 2.052 (7) Å in $PtCl_3$(2,6-Me_2py)$^-$,[15b] both of which suggest that steric effects, stemming from small ortho substituents on the pyridine, are not by themselves sufficient for a lengthening of the Pt–N bond. However, for *trans*-$PtCl_2$(**1a**)(PEt_3), with a coordinated bulky quinoline, the Pt–N separation is quite long at 2.155 (13) Å.[6] Consequently, the Pt–N separations in this work could arise from a combination of steric and electronic effects, the latter due to having $AsEt_3$ or PEt_3 trans to the coordinated pyridine nitrogen. We note that the Pt–N bond distance in our model complex, at 2.155 (5) Å, is slightly longer than the same bond in $PtCl_2$(**2h**)($AsEt_3$) but is almost identical with that in *trans*-$PtCl_2$(**1a**)(PEt_3), 2.160 (2) Å, and attribute this to PEt_3 having a larger trans influence than $AsEt_3$.[6] In any case, the bond distances and angles in *trans*-$PtCl_2$(**2h**)($AsEt_3$)$_2$ are reasonable and do not suggest that the large organic Schiff base disturbs the local coordination sphere to a major extent.

The pyridine moiety in the Pt complex is not planar with respect to the coordination plane. The observed 72° twist probably stems, once again, from both steric and electronic factors since there is no obvious steric reason preventing an angle of ca. 90°. In view of the torsion angles found in the complexes $PtCl_2$(4-Mepy)(styr),[14] 44°, *cis*-$PtCl_2(py)_2$],[12] 56 and 62°, *trans*-$PtCl_2$(py)(Me_2SO),[13] 59°, *trans*-$PtCl_2$(2-Mepy)(Me_2SO),[17] 72°, and *trans*-$PtCl_2$-(DMF)(2,6-Me_2py),[15] 88°, it would seem that pyridine type ligands are attempting to find the optimum orientation for p_π-d_π bonding involving the pseudo d_{xy}, d_{xz}, and d_{yz} orbitals and the ligand π-system. The complexes with 2- and 6-methyl substituents force a larger twist. The angle of 59° formed by the pyridine plane and the coordination plane in our model, *trans*-$PdCl_2$(2-NH_2-3-Mepy)(PEt_3), is quite consistent with this suggestion. This

(7) Bennett, M. J.; Cotton, F. A.; Weaver, D. L.; Williams, R. J.; Watson, W. J. *Acta Crystallogr.* **1967**, *23*, 788.
(8) Binamira-Soriaga, E.; Lundeen, M.; Seff, K. *J. Cryst. Mol. Struct.* **1979**, *9*, 67.
(9) Ferguson, G.; MaGrindle, R.; McAlees, A.; Parvez, M. *Acta Crystallogr., Sect. B: Struct. Crystallogr. Cryst. Chem.* **1982**, *B38*, 2679.
(10) Sin, G. A.; Sutton, L. E. *Molecular Structure by Diffraction Methods*, The Chemical Society: London, 1973; Vol. 1, p 606.
(11) Albinati, A.; Moriyama, H.; Rüegger, H.; Pregosin, P. S.; Togni, A. *Inorg. Chem.* **1985**, *24*, 4430.
(12) Colamarino, P.; Arioli, P. L. *J. Chem. Soc., Dalton Trans.* **1975**, 1656.
(13) Caruso, F.; Spagna, R.; Zambonelli, L. *Acta Crystallogr., Sect. B: Struct. Crystallogr. Cryst. Chem.* **1980**, *B36*, 713.
(14) Nyburg, S. C.; Simpson, K.; Wong-Nu, W. *J. Chem. Soc., Dalton Trans.* **1976**, 1865.
(15) (a) Rochon, F. D.; Kong, P. C.; Melanson, R. *Can. J. Chem.* **1980**, *58*, 97. (b) Rochon, F. D.; Melonson, R. *Acta Crystallogr., Sect. B: Struct. Crystallogr. Cryst. Chem.* **1980**, *B36*, 691.
(16) Motschi, H.; Pregosin, P. S. *Inorg. Chim. Acta* **1980**, *40*, 141. Motschi, H.; Pregosin, P. S.; Venanzi, L. M. *Helv. Chim. Acta* **1979**, *62*, 667.
(17) Melanson, R.; Rochon, F. *D. Acta Crystallogr. Sect. B: Struct. Crystallogr. Cryst. Chem.* **1978**, *B34*, 1125.

Table III. ^{1}H NMR[a] and IR[b] Data for the Ligands and Complexes[c]

L	J(Pt,H(7′))	δ(H(7′))	Δδ	δ(H(6))	Δδ	$\nu_{C=N}$	Δν
			$PtCl_2(L)AsEt_3$				
2a	8.4	9.54	0.07	8.61	0.29	1626	13
2b	10.3	9.52	0.34	8.63	0.30	1640	20
2c	10.6	9.48	0.26	8.64	0.31	1632	14
2d	9.8	9.31	0.26	8.61	0.30	1624	−3
2e	10.5	9.30	0.27	8.60	0.30		
2f	11.0	9.48	0.04	8.66	0.31		
2g	11.9	9.65	0.27	8.70	0.42	1625	23
2h	11.2	9.79	0.30	8.60	0.24		
			$PtCl_2(L)PEt_3$				
2a	7.7	9.49	0.02	8.53	0.21		
2b	9.6	9.42	0.24	8.57	0.25		
			$PdCl_2(L)PEt_3$				
2a		9.52	0.05	8.53	0.21	1628	15
2b		9.44	0.26	8.57	0.25	1645	25
2c		9.38	0.16	8.53	0.20	1632	14
2d		9.21	0.16	8.49	0.18	1625	−2
2f		9.43	−0.01	8.56	0.21	1622	12
2g		9.59	0.21	8.58	0.30	1620	18
2h		9.69	0.20	8.49	0.15		

[a] Chemical shifts in ppm, coupling constants in Hz, $CDCl_3$ solutions, Δ = (δ(complex) − δ(ligand)). [b] In cm^{-1} Δ = ($\nu_{complex} - \nu_{ligand}$). [c] Trans geometry.

pyridine moiety, which is smaller than that in **2h**, is not rotated as far from the coordination plane.

In our Schiff base complex, rotation about the Pt–N(1) bond brings the imine function into position for interaction with the metal. Indeed, the refined Pt–H distance is 2.43 (8) Å. This is consistent with both our observation for *trans*-$PtCl_2$(**1a**)(PEt_3),[6] 2.6 (1) Å, and with the literature value found for $PtCl_2$-$(PhCH{=}NMe)_2$,[18] 2.44 Å. Consequently, a potential geometric boundary condition for a Pt←H–C interaction has been fulfilled.

Before turning to the solution experiments, we note several additional structural aspects of coordinated **2h**: (a) the substituents on the imine carbon and nitrogen atoms are trans, (b) the torsion angle N(1)–C(2)–N(2)–C(7′) is ca. 50°, (c) the torsion angle N(2)–C(7′)–C(7)–C(8) is −177°, and (d) the C=N bond separation, 1.238 (11) Å, is consistent with that for a normal imine.

B. NMR Spectroscopy. (a) ^{1}H NMR. The most interesting aspect of the ^{1}H NMR data arises from the coupling of the imine proton to the platinum-195. The observed 7.7–11.9 Hz range shown in Table III is similar if slightly smaller than that found for the coordinated quinolines **1**, and confirms that, geometry permitting, weak covalent interactions between a proximate hydrogen and platinum are possible. The aryl substituent, R, does affect J(Pt,H) slightly, with the most prominent change arising from the 2-NO_2 substituent on the ring. The ^{1}H chemical shift of the imine proton moves to low field on complexation by 0.04–0.34 ppm. (For $PdCl_2$(**1f**)(PEt_3), the shift is 0.01 ppm to high field.) This is modest compared to the 1.62 ppm low-field shift found for $PtCl_2$(**1a**)(PEt_3). Most of the imine ^{1}H Δδ values fall in the narrow range 0.26–0.34 ppm (Δδ = δ(complex) − δ(ligand).

The coordination chemical shifts for the protons ortho to the pyridine nitrogen, H(6), are somewhat larger, 0.15–0.42 ppm, and most likely derive from a combination of electronic and anisotropic effects, the former related to the partial positive charge on nitrogen due to coordination and the latter stemming from the cis Pt–Cl bond.

The aryl methyl proton resonances at C(3) all shift upfield by 0.09–0.23 ppm, and we believe this comes from rotation about the C(2)–N(imine) bond, thereby moderating the deshielding influence of the imine nitrogen lone pair. We note that the hydroxyl protons in **2f** and **2g** are intramolecularly hydrogen bound, in both the ligands and their complexes, as exhibited by their very low-field positions.

(18) Kuzinina, L. G.; Strukhov, Y. T. *Cryst. Struct. Commun.* **1979**, *8*, 715.

Table IV. ^{13}C and ^{31}P NMR Data[a] for the Complexes

L	δ(^{13}C(7′))	Δδ	δ(^{13}C(6))	Δδ	δ(^{31}P)[b]
		$PtCl_2(L)AsEt_3$			
2a	163.6	4.6	147.7	1.0	
2b	165.0	5.9	147.9	1.4	
2c	164.9	5.8	147.4	0.9	
2d	165.7	5.3	147.2	0.8	
2e	166.3	5.9	147.7	1.4	
2f	170.5	6.3	148.2	1.7	
2g	170.6	7.2	148.3	1.9	
2h	166.5	4.4	147.5	1.1	
		$PtCl_2(L)PEt_3$			
2a	163.5	4.5	147.3	0.6	−1.2 [3458]
2b	165.0	5.9	147.4	0.9	−1.2 [3467]
		$PdCl_2(L)PEt_3$			
2a	162.9	3.9	147.1	0.4	35.1
2b	164.7	5.6	147.3	0.8	34.7
2c	165.0	5.9	147.3	0.8	35.6
2d	165.3	4.9	146.5	0.1	
2f	169.8	5.6	147.0	0.5	36.3
2g	169.7	6.3	147.0	0.6	36.6

[a] Chemical shifts in ppm, $CDCl_3$ solutions. [b] Relative to external H_3PO_4; negative sign = to high field of the reference ^1J(Pt,P) in brackets (in Hz).

(b) ^{13}C NMR. As seen from Table IV, the imine carbon resonance (C(7′)) for *trans*-$PtCl_2$(**2**)$AsEt_3$ experiences a 4–7 ppm downfield shift on complexation, which, although modest, is larger than the <2 ppm low-field shift for the carbon adjacent to the pyridine nitrogen but comparable to that found for C(2) attached to both nitrogens (ca. 2.5–6.5 ppm). In view of the possibility of cumulative minor changes in δ(^{13}C) from coordination, rotation, and local anisotropic effects, we are not in a position to attribute the Δδ values for C(7′) to a metal-related effect. We have also obtained ^1J\{^{13}C(7′), ^{1}H(7′)\} values for **2e** and its platinum complex and find these to be identical, within experimental error. This is consistent with our previous observation[6a] for **1** and its complex so that for **2**, as well, there is no compelling evidence for a change in hybridization at C(7′) due to complexation (we note from the crystallography that the N(2)–C(7′)–C(7) angle is 125°). The carbon resonances of the methyl groups change position by <0.6 ppm, and we take this as support for our contention with regard to their respective proton shifts.

We had hoped that we could empirically extract an NMR probe that would be useful for defining a Pd←H–C interaction in our palladium complexes; however, as shown by both the ^{1}H and ^{13}C data, this is not the case. These Δδ values are similar to those of the platinum analogues but remain unconvincing.

Comments. It is conceivable that the direction of the ligand C–H vector, with respect to the metal, plays a crucial role in determining the size of ^nJ(Pt,H). The nature of the C–H bond is also important for J(Pt,H).

For both **1a** and **2h** rotation about the pyridine nitrogen–platinum bond relieves steric strain and brings the C–H bond into position. The 3-methyl group in **2h** contributes toward holding the imine function in the general area of the metal by preventing rotation past the C(3)–CH_3 bond. Complex **4**, in which we find[5]

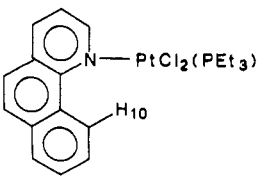

4

an 8.4-Hz ^nJ(Pt,H(10))value, is also rigid with respect to C(10)–H(10) rotation. Naturally, not all potentially suitable 2-substituted pyridines show this type of coupling. Consider the model complexes **5** and **6**. If these molecules (easily prepared from the respective dimers and 2 equiv of the commercially available ligands) existed solely as shown we would expect a

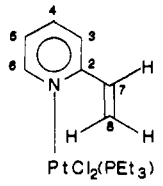

5

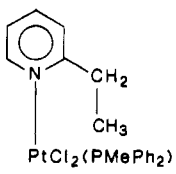

6

significant J(Pt,H) coupling to both $H(8)_{syn}$ and the CH_3 protons, respectively. We do not observe either of these spin–spin interactions, although coupling constants to H(7), 6.7 Hz, and CH_2, ca. 7 Hz, are detected. Presumably rotation about the C(2)–C(7) and C(2)–CH_2 axes are responsible for minimizing the contact. For $PtCl_2$(**2h**)($AsEt_3$), J(Pt,H) = 11.2 Hz, whereas for $PtCl_2$(**1a**)(PEt_3) the corresponding coupling constant is 13.7 Hz. The values for $PtCl_2$(**1a**)($AsEt_3$) and $PtCl_2$(**2b**)(PEt_3) are 15.4 and 9.6 Hz, respectively. Thus for the same trans ligand **1a** gives slightly larger values than does **2**.

We conclude that the ligand **2** is also suitable for coordinating Pt(II) in such a way as to bring the imine hydrogen close to the metal. This results in a weak Pt←H–C interaction, which we monitor in the form of a J(Pt,H) coupling constant. The magnitude of this spin–spin interaction is only a few percent of that expected for a bridging platinum hydride complex[19,20] so that we feel justified once again[6b] in suggesting that this M←H–C interaction is different from that formulated as an "agostic" covalent bond. Moreover, we show that the electronic effects promulgated through the benzene ring do influence the platinum–proton coupling, but only slightly. Indeed, the effect is smaller than that due to ligand size in the complexes $PtCl_2$(**1a**)(tertiary arsine).[6b] There are indications that proximity to the metal, in terms of restricted rotational possibilities, may prove important for our novel ^nJ(Pt,H) interactions.

Experimental Section

Crystals suitable for x-ray diffraction of *trans*-$PtCl_2$(**2h**)($AsEt_3$) were obtained by crystallization from CH_2Cl_2/hexane at ca. −20 °C as were those of $PdCl_2$(2-NH_2-3-Mepy)(PEt_3). Data were collected at room temperature (for both compounds) on a Nonius CAD4 automatic diffractometer by using the parameters listed in Table V, with variable scan speed, to obtain constant statistical precision on the collected intensities. Data were corrected for Lorentz and polarization factors and absorption with the data reduction programs of the CAD4-SDP package.[21] Intensities were considered as observed if $F_o \geq 2.5\sigma F_o$, while an $I_{net} = 0.0$ was given to those reflections having negative net intensities. The structures were solved by a combination of Patterson and Fourier methods and refined by a block-diagonal least-squares procedure[22] (the function minimized is $(\sum W(|F_o| - 1/k|F_c|)^2)$ with weights obtained from a Cruickshank scheme,[23] by demanding that no trend is present in the weights with $|F_o|$ or $(\sin\theta)/\lambda$. No extinction correction was deemed necessary for both sets of data. The scattering factors used were taken from ref[24], and a correction for the real and imaginary part of the anomalous dispersion was taken into account, by using tabulated values.[24]

Structural Studies. A. *trans*-$PtCl_2$(2h)($AsEt_3$). Crystals of the complex have prismatic habits and are air-stable. A crystal was mounted on a glass fiber for the data collection. Cell constants were obtained by a least-squares fit of 23 high-angle reflections ($11.0 \leq \theta \leq 35.0$) using the CAD4 centering routines. Crystallographic data and data collection parameters are given parameters are given in Table V. Three standard reflections ($3\bar{3}\bar{1}$, $2\bar{2}5$, $4\bar{1}4$) were measured every hour and used to check the stability of the crystal and of the experimental conditions; no significant variation was detected. The orientation of the crystal was checked by measuring three reflections ($1\bar{3}\bar{3}$, $4\bar{1}1$, $4\bar{1}4$) every 300. An empirical absorption correction was applied by using the azimuthal (Ψ) scans of the high χ angle reflections: 312; 412; 514. Transmission factors

Table V. Experimental Data for the X-ray Diffraction Studies

formula	$PtCl_2AsN_2C_{22}H_{23}$	$PdCl_2PN_2C_{12}H_{23}$
M_r	656.36	403.61
cryst dimens, mm	0.2 × 0.2 × 0.3	0.25 × 0.25 × 0.15
space group	$P\bar{1}$	Cc
a, Å	8.177 (2)	13.866 (1)
b, Å	10.832 (1)	7.597 (1)
c, Å	15.370 (2)	16.555 (1)
α, deg	82.99 (2)	
β, deg	81.29 (2)	101.974 (3)
γ, deg	89.41 (2)	
V, Å^3	1248.7 (8)	1705.96 (6)
Z	2	4
ρ(calcd), g cm^{-3}	1.74	1.57
radiation	*d*	d
measd reflcns[a]	$\pm h,\pm k,+l$	$\pm h,+k,+l$
μ, cm^{-1}	72.2	14.7
2θ range, deg	$4.5 \leq 2\theta \leq 50.0$	$5.0 \leq 2\theta \leq 52.0$
scan type	$\omega/2\theta$	$\omega/2\theta$
max scan speed, deg min^{-1}	20.0	20.0
scan width, deg	1.10 + 0.35 tan θ	1.00 + 0.35 tan θ
max counting time, sec	56	60
prescan rejectn limit	0.5 (2σ)	0.5 (2σ)
prescan accept limit	0.03 (33σ)	0.03 (33σ)
bkgd time, s	0.5 × (scan time)	0.5 × (scan time)
receiving aperture		
horiz, mm	1.85 + tan θ	1.85 + tan θ
vert, mm	4.0	4.0
no. of indept data	4374	1681
no. of obsd data $[F_o > 2.5\sigma(F_o)]$	3584	1466
R[b]	0.037	0.028
R_w[c]	0.045	0.032

[a] Collected at room temperature. [b] $R = \sum[|F_o| - |F_c|]/\sum|F_o|$. [c] $R_w = [\sum w(|F_o| - |F_c|)^2/\sum wF_o^2]^{1/2}$. [d] Mo K$\alpha$ graphite monochromated; λ = 0.710 69 Å.

Table VI. Final Positional Parameters for *trans*-$PtCl_2$(**2h**)($AsEt_3$)

	x/a	*y/b*	*z/c*
Pt	0.23756 (4)	0.14762 (3)	0.16273 (2)
As	0.4620 (1)	0.0524 (1)	0.2252 (1)
Cl(1)	0.4033 (3)	0.3159 (3)	0.0997 (2)
Cl(2)	0.0649 (4)	−0.0206 (3)	0.2213 (2)
N(1)	0.0449 (9)	0.2373 (7)	0.1003 (5)
C(2)	−0.0301 (10)	0.3405 (8)	0.1273 (6)
C(3)	−0.1476 (10)	0.4036 (8)	0.0780 (7)
C(4)	−0.1850 (12)	0.3527 (12)	−0.0005 (7)
C(5)	−0.1079 (11)	0.2497 (10)	−0.0281 (6)
C(6)	0.0058 (12)	0.1923 (10)	0.0220 (6)
N(2)	0.0167 (9)	0.3913 (6)	0.2053 (5)
C(7)	0.0225 (11)	0.3207 (8)	0.2792 (6)
C(7)	0.0839 (11)	0.3564 (9)	0.3657 (7)
C(8)	0.0506 (12)	0.2731 (9)	0.4489 (7)
C(9)	0.1101 (15)	0.3028 (12)	0.5285 (7)
C(10)	0.2023 (14)	0.4070 (13)	0.5286 (7)
C(11)	0.2346 (14)	0.4857 (11)	0.4469 (9)
C(2)	0.1802 (12)	0.4663 (10)	0.3626 (9)
C(13)	−0.2350 (13)	0.5140 (10)	0.1129 (7)
C(14)	−0.0511 (18)	0.1610 (15)	0.4554 (9)
C(15)	0.2658 (16)	0.4356 (14)	0.6166 (9)
C(16)	0.2286 (18)	0.5549 (12)	0.2761 (10)
C(17As)	0.6208 (12)	0.1642 (12)	0.2590 (9)p
C(18As)	0.5402 (19)	0.2462 (14)	0.3298 (12)
C(19As)	0.4008 (15)	−0.0612 (12)	0.3401 (9)
C(20As)	0.5480 (23)	−0.1129 (16)	0.3862 (12)
C(21As)	0.6031 (14)	−0.0419 (15)	0.1361 (10)
C(22As)	0.519 (25)	−0.1534 (18)	0.1178 (15)
H(C6)	0.0186 (97)	−0.2278 (73)	0.2720 (54)

(19) Carmona, D.; Chalopupka, S.; Jans, J.; Thouvenot, R.; Venanzi, L. M. *J. Organomet. Chem.* **1984**, *275*, 303. Carmona, D.; Thouvenot, R.; Venanzi, L. M.; Bachechi, F.; Zambonelli, L. *J. Organomet. Chem.* **1983**, *259*, 589. Boron, P.; Musco, A.; Venanzi, L. M.; *Inorg. Chem.* **1982**, *21*, 4192. Albinati, A.; Naegeli, R.; Togni, A.; Venanzi, L. M. *Organometallics* **1983**, *2*, 926.

(20) Pregosin, P. S.; Togni, A.; Venanzi, L. M. *Angew. Chem. Int. Ed. Engl.* **1981**, *20*, 668. Immirzi, A.; Musco, A.; Pregosin, P. S.; Venanzi, L. M. *Angew. Chem., Int. Ed. Engl.* **1980**, *19*, 721.

(21) *Enraf-Nonius Structure Determination Package (SDP)*; Enraf-Nonius: Delft, Holland, 1980.

(22) For references to least-squares Fourier and structure factors calculation programs, see: Albinati, A.; Bruckner, S. *Acta Crystallogr. Sect. B: Struct. Crystallogr. Cryst. Chem.* **1978**, *B34*, 3390.

(23) Cruickshank, D. W. J. In *Crystallographic Computing*; Ahmed F. R., Ed.; Munksgaard: Copenhagen, 1970.

(24) *International Tables for X-ray Crystallography*; Kynoch: Birmingham, England, 1974; Vol. IV.

Table VII. Final Positional Parameters for *trans*-$PdCl_2(2\text{-}NH_2\text{-}3\text{-}Mepy)(PEt_3)$

	x/a	*y/b*	*z/c*
Pd	0.00000 (0)	−0.00620 (5)	0.25000 (0)
Cl(1)	−0.1384 (1)	−0.0951 (3)	0.1567 (1)
Cl(2)	0.1364 (1)	0.0625 (3)	0.3497 (1)
P	0.0890 (1)	−0.0981 (2)	0.1605 (1)
N(1)	−0.0870 (4)	0.0948 (7)	0.3335 (3)
C(2)	−0.1520 (5)	0.0018 (7)	0.3657 (4)
C(3)	−0.2051 (5)	0.0835 (10)	0.4203 (3)
C(4)	−0.1879 (6)	0.2558 (10)	0.4402 (4)
C(5)	0.1193 (6)	0.3494 (9)	0.4080 (5)
C(6)	−0.0696 (5)	0.2665 (9)	0.3549 (4)
N(2)	0.1647 (4)	0.1697 (7)	0.3456 (4)
C(7)	−0.2792 (7)	0.0226 (12)	0.4544 (6)
C(1P)	0.0453 (7)	−0.0127 (10)	0.0568 (5)
C(2P)	0.0419 (8)	0.1874 (14)	0.0525 (7)
C(3P)	0.2193 (5)	−0.0411 (12)	0.1888 (5)
C(4P)	0.2830 (6)	−0.1013 (13)	0.1293 (6)
C(5P)	0.0796 (7)	−0.3330 (10)	0.1465 (5)
C(6P)	0.1016 (10)	−0.4349 (14)	0.2254 (7)

were in the range 0.64–0.99. The structure was refined by block-diagonal least-squares techniques as described above with anisotropic temperature factors used for all atoms. Toward the end of the refinement a strong peak, in an acceptable position for the H atom bound to C(6), was clearly visible and was therefore included in the refined model with an isotropic temperature factor; the contributions of the other hydrogen atoms in their idealized positions (C–H bond lengths = 0.95 Å, B_{iso} = 6.5 Å^2) were also taken into account but not refined. Upon convergence (no shifts $\geq 0.5\ \sigma$) the last Fourier difference map showed no significant features. Final positional parameters are listed in Table VI. Tables of thermal factors (Table S1) and F_o and F_c (Table S2) and a complete list of bond distances and angles (Table S3) are given in the supplementary material.

B. *trans*-$PdCl_2(2\text{-}NH_2\text{-}3\text{-}Mepy)(PEt_3)$. Crystals of the complex have an irregular tabular habit and are air-stable. A small crystal (0.25 × 0.25 × 0.15 maximum dimensions) was chosen for the data collection and mounted on a glass fiber at random orientation. Systematic absences were consistent with space groups *Cc* or *C*2/*c*, the latter (from the density) requiring the molecule to lie on a crystallographic symmetry element. Cell constants were obtained by a least-squares fit of the 2θ values of 25 high-angle reflections ($10.5 \leq \theta \leq 12.5$) using the CAD4 centering routine. Crystallographic data and data collection parameters are listed in Table V. Three standard reflections were measured every hour (1,1,10; 516; $\bar{5}1\bar{6}$) to check the stability of the crystal and of the experimental conditions: no significant variation or decay was observed. The orientation of the crystal was monitored every 300 reflections by centering three reflections: $\bar{4}28$; $\bar{5}1\bar{6}$; 516. An empirical absorption correction was applied by using Ψ scans of the following reflections: 402; 602; 604; 10, 0, 4. Transmission factors were in the range 0.982–0.988. The structure was refined by block-diagonal least-squares techniques as described above, with anisotropic temperature factors used for all atoms but the hydrogens; the contribution of the hydrogen atoms in their calculated positions (C–H bond lengths = 0.95 Å, B_{iso} = 6.0 Å^2) was taken into account but not refined. A refinement in the centrosymmetric space group with a disordered model for the organic ligands imposed by a crystallographic 2-fold axis did not give a significantly better *R* factor according to the Hamilton test;[25a] therefore, the original choice of the acentric *Cc* space group was retained. Upon convergence (no shifts $>0.4\sigma$) the last Fourier difference map showed no significant features. Final positional parameters are listed in Table VII (the handedness of the crystal was tested by refining each of the two enantiomorph sets of coordinates; those listed gave the lower *R* factor).[25b] Tables of anisotropic thermal factors, observed and calcdulated structure factors, and an extensive list of bond lengths and angles are given in the supplementary material (Tables S4–S6).

Table VIII. Microanalytical Data for the Complexes

L	found (calcd) % C	% H	% N
	$PtCl_2(L)AsEt_3$		
2a	33.98 (34.09)	3.94 (3.92)	6.13 (6.28)
2b	33.82 (34.09)	3.93 (3.92)	6.29 (6.28)
2c	34.16 (34.09)	3.86 (3.92)	6.21 (6.28)
2d	34.45 (34.64)	3.93 (3.98)	4.30 (4.25)
2f	35.62 (35.63)	4.28 (4.22)	4.64 (4.38)
2g	35.74 (35.83)	4.38 (4.36)	4.07 (4.18)
2h	39.47 (39.65)	4.96 (4.99)	4.41 (4.20)
	$PtCl_2(L)PEt_3$		
2a	36.41 (36.49)	4.03 (4.19)	6.45 (6.72)
2b	36.22 (36.49)	4.23 (4.19)	6.61 (6.72)
	$PdCl_2(L)(PEt_3)$		
2a	42.48 (42.52)	4.89 (4.88)	7.77 (7.83)
2b	42.43 (42.52)	4.87 (4.88)	7.63 (7.83)
2c	42.54 (42.52)	4.89 (4.88)	7.79 (7.83)
2d	43.85 (43.37)	5.24 (4.98)	5.42 (5.32)
2f	44.80 (44.95)	5.38 (5.36)	5.36 (5.52)
2g	44.59 (44.67)	5.61 (5.44)	5.32 (5.21)
2h	49.26 (49.50)	6.12 (6.23)	5.15 (5.25)

2-Amino-3-methylpyridine was available from Fluka, Buchs. The Schiff base was prepared by condensing 1 equiv of the corresponding benzaldehyde with the aminopyridine to give **2**. All of the complexes were prepared by reacting 2 equiv of ligand **2** with 1 equiv of the dimer $[Pt(\mu\text{-}Cl)ClL]_2$ in CH_2Cl_2 or $CHCl_3$. Yields are essentially quantitative with losses arising from recrystallization (CH_2Cl_2/hexane). Microanalytical data for some of the complexes are shown in Table VIII.

NMR spectra were measured on Bruker WM-250 and WH-90 spectrometers. $^n J$(Pt,H) values are best measured on the lower field machine.[5] The data were obtained from $CDCl_3$ solutions at room temperature. IR spectra were measured as KBr or CsBr pellets on a Perkin-Elmer Series 1430 spectrometer.

Acknowledgment. We thank the Swiss National Science Foundation and Ciba-Geigy, Basel, Switzerland, for support (C.A.) and the Johnson-Matthey Research Centre, England, for the loan of platinum metals.

Supplementary Material Available: Tables of thermal factors (Tables S1 and S4) and an extensive list of bond lengths and angles (Tables S3 and S6) (8 pages); tables of structure factors (Tables S2 and S5) (34 pages). Ordering information is given on any current masthead page.

(25) (a) Hamilton, W. C. *Acta Crystallogr.* **1965**, *18*, 502. (b) Ibers, J.; Hamilton, E. C. *Acta Crystallogr.* **1964**, *17*, 781.